

Impact-Induced Melting by Giant Collision Events

L. Manske^{1,2}, K. Wünnemann^{1,2}, ¹Museum für Naturkunde, Leibniz Institut for Evolution and Biodiversity Science, 10115 Berlin, Germany, lukas.manske@mfn-berlin.de, ²Institute for Geological Sciences, Planetary Sciences and Remote Sensing, Freie Universität 12249 Berlin, Germany

1. Introduction

We have carried out a series of numerical models to investigate the generation of impact-induced melt onto the terrestrial planets due to collisions with asteroids larger than 1 km in diameter, which may not be accurately addressed by classical scaling-laws [1,2]. During the accretion phase, the thermochemical evolution of the terrestrial planets was heavily influenced by giant collisions with other cosmic bodies such as the Moon-forming event on the young Earth [3]. Besides variations in the compositional budget, such impacts transfer a significant amount of energy to heat up the planet and cause the formation of local magma ponds or even global magma oceans. The amount of impact-induced melt can be predicted by scaling-laws [1,2]. However, scaling laws neither account for the interior structure of a differentiated planet nor for the initial temperature or lithostatic pressure of planets interior. This is negligible for smaller scale impacts (smaller than basin forming impacts), but on a larger scale they are not sufficiently accurate, especially when the initial temperatures are close to the solidus (younger planet). In addition, scaling laws can neither predict decompression melting nor locate distribution of the melt post impact. To better understand and quantify the mechanism of heat production and locate melting during and right after large-scale impact events we have conducted a series of numerical models and determined the volume of melt production.

2. Methods

To model hypervelocity collisions we use the iSALE Eulerian shock physics code [4,5] (Version *Dellen*). The thermodynamic state (EoS) is calculated by ANEOS [6] for basalt/granite, dunite, and iron representing the planetary crust, mantle and core, respectively.

To determine the distribution and volume of impact-induced melting we calculate the local, (post-impact) final temperature T_f via the peak shock pressure method [2,7]; to assess whether the material

is (partially) molten or not, we compare T_f with the solidus and liquidus temperature $T_{S/L}$ [8]. As the method relies on Lagrangian tracers, which track the movement of the material, this approach allows for taking decompression melting into account. Decompression is a consequence of displacement of material in the course of crater formation resulting in a lower lithostatic pressure of a given mass unit after crater formation than before impact. We assume that the Moon and Martian crust consists of basalt whereas the Earth's crust is formed by granite. The planets mantle and the impactors are modeled with dunite. Differentiated impactors are neglected at this stage. We consider two different initial thermal profiles T_i representing young (hot) and old (cold) planets as shown in figure 1. In all models the projectile radius is resolved by 50 cells (50 CPPR). For very large impacts we account for the curvature of the target.

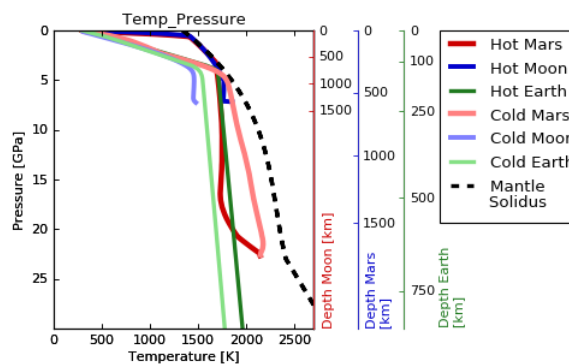


Figure 1: Initial temperature profiles for a young (Hot: dark color) and old (Cold: light color) Earth (green), Moon (blue) and Mars (red) [9]. The Solidus curve for mantle material (Duntie) is shown in black [8].

3. Results

In our model series, we vary the impactor diameter L and velocity v_i for different temperature conditions T_i (here only $v_i = 15$ km/s for Mars and Moon and $v_i = 17$ km/s for Earth is presented). For each simulation, we quantify melt volumes and locate the melt provenience and final distribution.

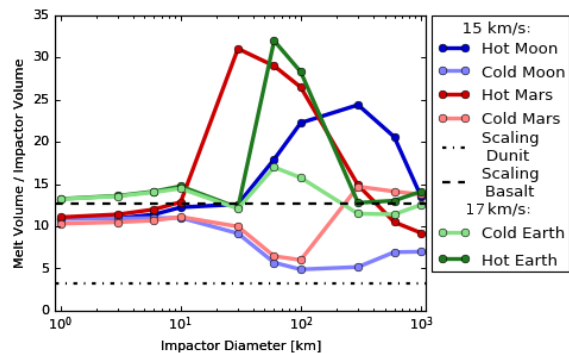


Figure 2: Normalized melt production for hot and cold planets. We show classical scaling laws for basalt [1] and dunitite [2] (dashed lines). Models for different planets are based on young (dark colors) and old (light colors) temperature profiles presented in figure 1.

Figure 2 shows the melt volume normalized by the projectile volume as a function of impactor diameter. The models agree with estimates from scaling-laws (dashed lines) for small scale impacts (up to 10 km impactor diameter). In this range the differentiated planet structure and thermal profiles do not affect melt production since the impactor only penetrates into the crust, where the temperature increase with depth is dominated by conduction. However, larger events are not well represented by scaling laws. We find that, for a given initial temperature T_i , when a certain impactor size is exceeded, the normalized melt production ($V_{melt}/V_{projectile}$) deviates significantly from the reference model and estimates from scaling laws. The distinct increase in melt production for impactors larger than 10 km in diameter for the hot planet scenarios is caused by the depth-dependence of ΔT_M , which is given by the difference between T_i and solidus (and liquidus) T_{LS} . It can be shown that the maximum normalized melt production occurs when the main melt region is located in the area at a depth where ΔT_M is very small. This area usually corresponds to the bottom of the lithosphere. However, if ΔT_M is large over the entire relevant depth range, like in the cold Moon scenario, melt production stays in agreement with the mantle scaling laws even for large scale impacts.

Figure 3 shows the post-impact distribution of partially molten material for a 10 km (a), a 30 km (b) and a 300 km (c) impactor diameter on Mars for a young/hot (left) and old/cold (right) target (cf. Fig. 1). For impactors larger than 10 km in diameter we find that the initial thermal target setup significantly

affects the final melt distribution and the crater morphology. For hotter and younger Mars (left), the final crater appears flatter and more melt is produced (cf. Fig. 2). Also the effect of mantle uplifting is more prominent compared to an older target (right).

The results of this study will be used to improve or derive scaling laws that are sensitive to planet structures and initial temperatures. Furthermore planetary evolution models (e.g. [3]) can be improved using the results of this study.

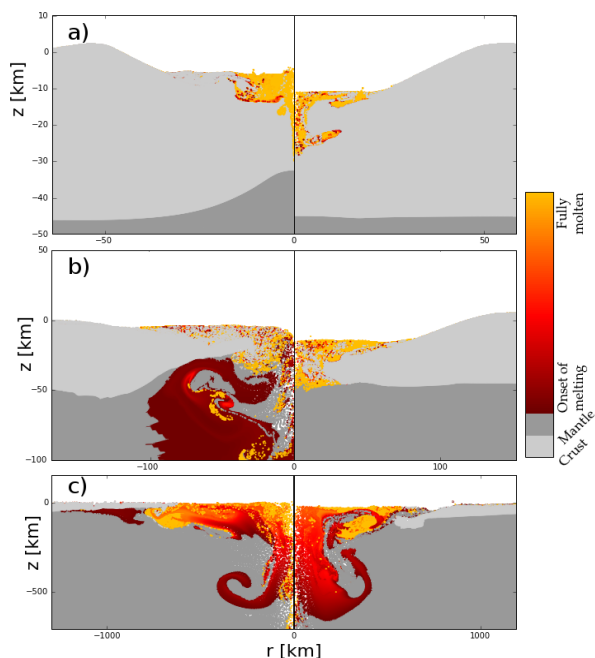


Figure 3: Post-impact melt distribution for a young (left) and old (right) Mars (cf. Fig. 1) with impactor diameters from 10 km (a) and 30 km (b) to 300 km (c) (cf. Fig. 2).

Colors indicate (partially) molten material.

4. Acknowledgements

We gratefully acknowledge the developers of iSALE, including Gareth Collins, Dirk Elbeshausen, Boris Ivanov and Jay Melosh. This work was funded by the Deutsche Forschungsgemeinschaft (SFB-TRR 170, Subproj. C2, C4).

5. References

- [1] Abramov O. et al. (2012) *Icarus* 218, 906-916.
- [2] Pierazzo et al. (1997) *Icarus* 127, 408-423, 1997.
- [3] Marchi S. et al. (2014) *Nature* 511, 578-582.
- [4] Collins. G. S. et al. (2004) *Meteoritics & Planet. Sci.* 39, 217-231.
- [5] Wünnemann K. et al. (2006) *Icarus* 180, 514-527.
- [6] Thompson and Lauson (1972) Report SC-RR-71 0714, Sandia National Lab.
- [7] Ruedas, T. and Breuer, D. (2017) *JGR*, 122, 1554-1579
- [8] Plesa, A.-C. et al. (2016) *JGR* 121, 2386-2403.
- [9] Manske L. et al., 49th LPSC (2018), Abstract #2269.